Am J Transl Res 2019;11(2):1030-1039
www.ajtr.org /ISSN:1943-8141/AJTR0078591

Original Article

JQ1 effectively inhibits vasculogenic mimicry of pancreatic ductal adenocarcinoma cells via the ERK1/2-MMP-2/9 signaling pathway both in vitro and in vivo

Meng Zhuo[1*], Cuncun Yuan[2*], Ting Han[1*], Hai Hu[3], Jiujie Cui[1], Feng Jiao[1*], Liwei Wang[1*]

[1]Department of Oncology, State Key Laboratory for Oncogenes and Related Genes, Renji Hospital, School of Medicine, Shanghai Jiaotong University, Shanghai Cancer Institute, Shanghai 200127, China; [2]Department of Pathology, Eye & ENT Hospital of Fudan University, 83 Fenyang Road, Shanghai 201114, P. R. China; [3]Department of Medical Oncology and Pancreatic Cancer Center, Shanghai General Hospital, School of Medicine, Shanghai Jiao Tong University, Shanghai, P. R. China. [*]Equal contributors.

Received April 26, 2018; Accepted December 23, 2018; Epub February 15, 2019; Published February 28, 2019

Abstract: Vasculogenic mimicry (VM) is an alternative type of blood and nutrition supply that is associated with more aggressive tumor biology and increased cancer-related mortality. However, the clinical implications of VM remain unclear in patients with pancreatic ductal adenocarcinoma (PDAC). The aim of this study was to investigate the clinical significance of VM in PDAC patients and to seek a novel and more efficient treatment strategy by targeting this unique process. Here, cluster of differentiation 34 (CD34)/periodic acid-Schiff (PAS) double-staining of 76 PDAC clinical specimens revealed that VM expression was related to clinical stage (P=0.049) and lymph node metastasis (P=0.023). Notably, VM expression was correlated with a poor prognosis in patients with PDAC. Additionally, we discovered that there was a positive correlation between the expressions of VM and phosphorylated extracellular signal regulated kinase (p-ERK1/2) in 76 clinical samples (P<0.001). Moreover, our results further indicated that treatment with the ERK1/2 inhibitor SCH772984 effectively blocked VM formation by repressing the production of p-ERK1/2-MMP-2/9, which have been established as classical markers of VM. Further, JQ1, a bromodomain and extraterminal domain (BET) inhibitor, also exerted significant inhibitory efficiency against VM formation by decreasing the activation of ERK1/2-MMP-2/9. In conclusion, our work suggests that VM is a marker of poor prognosis in patients with PDAC and that JQ1 can inhibit VM formation via the ERK1/2-MMP-2/9 signaling pathway.

Keywords: Pancreatic ductal adenocarcinoma, vasculogenic mimicry, JQ1, ERK1/2, MMP-2/9

Introduction

Pancreatic ductal adenocarcinoma (PDAC) deaths primarily result from tumor metastases that are resistant to chemoradiotherapy [1]. Indeed, the accepted tenant underlying tumor survival has been that a supply of blood and nutrition is necessary to maintain rapid growth and metastasis [2]. However, neoplastic angiogenesis research and clinical trials that have focused on inhibiting endothelial cells have shown moderate or even worse antitumor results in PDAC [3]. Accordingly, the disappointing results of clinical trials that have focused on antiangiogenesis therapy in PDAC have given us novel insights into other functional vessel-like forms that underlie the perfusion of tumors.

Vasculogenic mimicry (VM), a functionally patterned vessel-like channel structure that is formed directly from aggressive tumor cells rather than endothelial cells, may account for the failure of antivascular therapy [4]. As a supplementary form of angiogenesis, VM tubules could supply sufficient blood perfusion and nutrition to rapidly growing tumors [5]. Recently, VM has been reported to be associated with cancer progression and poor prognosis in various malignant tumors [6-8]. However, the rate of VM positivity in PDAC tissues is not clear, and the clinical significance of VM in PDAC remains uncertain.

Previous studies have shown that the ERK1/2 signaling pathway, which is responsible for can-

cer cell survival and metastasis, plays an important role in VM formation in various cancers [9-11]. Moreover, Matrix metalloprotease (MMPs), especially MMP-2, MMP-9 and MMP-14, also show a positive correlation with VM formation and participate in the key signaling pathway of VM formation [12, 13]. Therefore, the ERK1/2-MMPs signal pathway was closely involved in the course of VM. JQ1 belongs to the family of BET (bromodomain and extraterminal domain) inhibitors, which were developed to occupy the binding pockets of acetylated histones, leading to the release of BRDs (bromodomains) from chromatin and the inhibition of downstream signals [14]. Ana S. Leal et al. [15] reported that JQ1 inhibits tumor growth by regulating the cell cycle and apoptosis by inhibiting the expression of p-ERK1/2 in PDAC cells. However, the potential effects of JQ1 on VM and its interaction with p-ERK1/2-MMP2/9 of these effects have not been fully studied.

Our study showed that VM is an unfavorable prognostic indicator for patients with PDAC. Furthermore, we found that JQ1, a novel and efficient treatment strategy, can inhibit VM formation via the ERK1/2-MMP signaling pathways. Our observations suggested that developing strategies to suppress VM formation could be a promising therapeutic approach for PDAC.

Materials and methods

Antibodies and inhibitors

Matrigel basement membrane matrix was obtained from Corning (Corning Incorporated, Corning, NY, USA). The primary antibodies anti-p44/42 MAPK (ERK1/2), anti-Phospho-p44/42 MAPK (ERK1/2) (Thr202/Tyr204), anti-MMP-2 and anti-MMP-9 were all purchased from Cell Signaling Technology. The primary antibodies anti-CD34 and anti-GAPDH were purchased from Santa Cruz Biotechnology. (+)JQ1, a small-molecule inhibitor of BET, and SCH772984, an ERK1/2 inhibitor, were purchased from Selleck and dissolved in dimethyl sulfoxide (DMSO).

Cell lines

Human umbilical vein endothelial cells (HUVECs) and AsPC-1, BxPC-3 and CFPAC-1 cells were grown in RPMI-1640 (Corning) (from Gibco, Carlsbad, CA, USA), and PANC-1 cells were maintained in Dulbecco's modified Eagle's medium (DMEM) (Corning). SW1990 cells were cultured in L-15 (Corning), and Capan-1 cells were cultured in Iscove's modification of DMEM (Corning) supplemented with 10% fetal bovine serum (FBS). The cells were maintained in a humidified incubator at 37°C in the presence of 5% CO_2.

Patients and samples

This study was approved and supervised by the Ethics Committee of Renji Hospital, Shanghai Jiao Tong University School of Medicine. Written informed consent was obtained from all subjects. Seventy-six tissue samples were collected by the surgery department between January 2009 and December 2012. Tumor tissue samples and adjacent noncancerous controls were collected during surgery. The tissue samples were histopathologically confirmed and staged in accordance with the Union for International Cancer Control.

Cluster of differentiation 34 (CD34)-periodic acid-Schiff (PAS) dual staining

Anti-CD34 antibodies were applied to the sections at a dilution ratio of 1:100. Then, after CD34 immunohistochemical staining, the sections were stained with 0.5% PAS for 10 min. CD34-negative and PAS-positive (CD34-/PAS+) vascular-like structures were identified by the detection of PAS-positive loops surrounding tumor cells, but not endothelial cells, with or without red blood cells in the lumen. For further analysis, the PDAC specimens were divided into two groups, defined as "VM positive" and "VM negative", through detecting the expression of CD34-/PAS+ staining. The sections were viewed and subjected to careful identification by two trained pathologists.

Immunohistochemical staining (IHC) analysis

IHC staining for -p-ERK1/2 expression in PDAC tissues and subcutaneous tumor of tissues of xenografts was performed. Anti-p-ERK1/2 antibody was applied at 1:100. Comprehensive score = staining percentage × intensity, staining intensity was as follows: (0) negative, (1) weak, (2) moderate and (3) intense. The scoring for staining percentage was as follows: (0) 0%, (1) ≤ 25%, (2) 26-50%, (3) 51-75% and (4) ≥76. The final p-ERK expression was classified as follows: "low expression" (scores <6), "high ex-

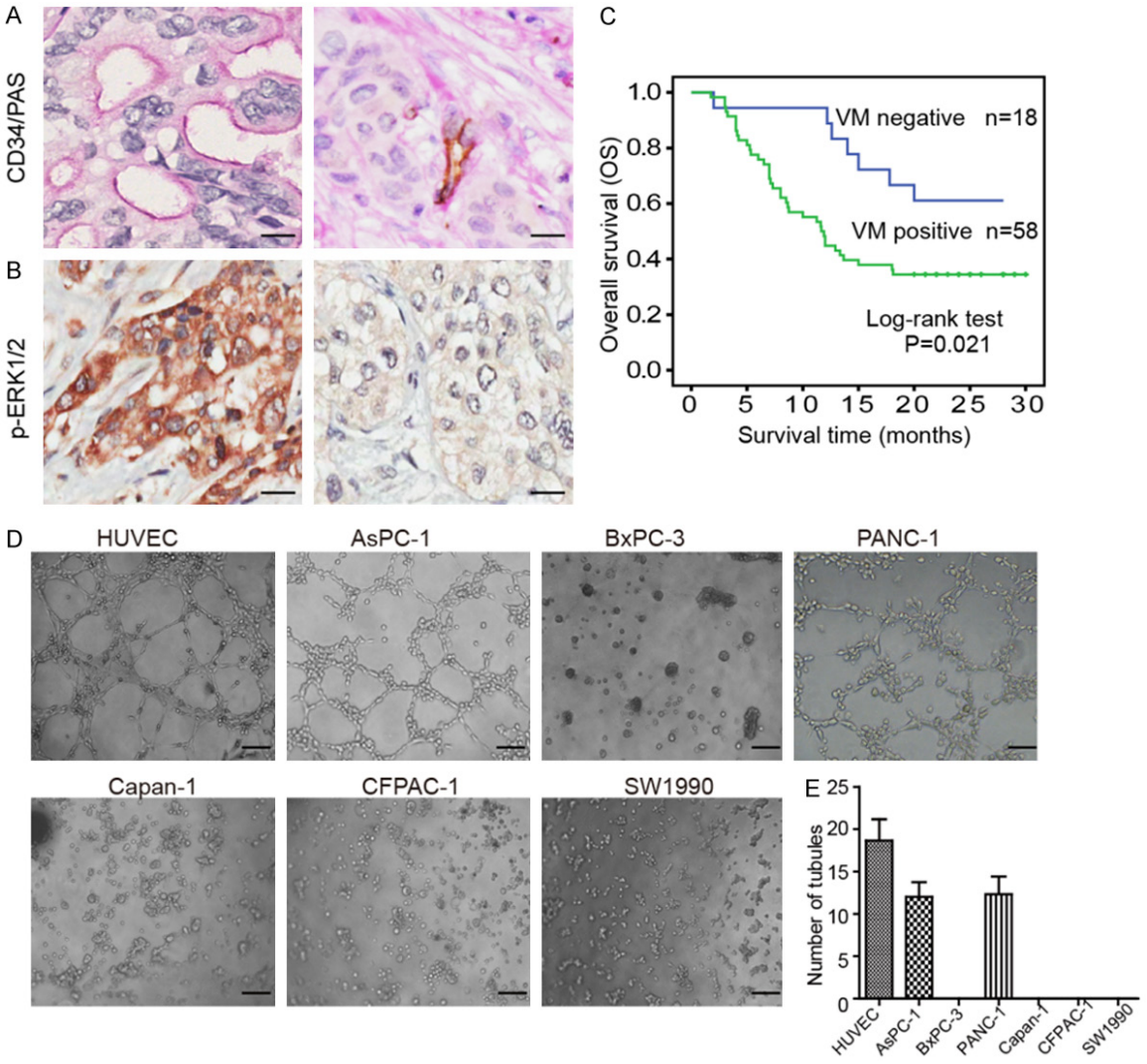

Figure 1. VM expression positively correlated p-ERK1/2 and predicts poor prognosis in PDAC samples. CD34/PAS dual staining and IHC were performed in 76 PDAC tissue specimens. A. CD34/PAS double-staining demonstrated that VM channels, lined with tumor cells, were CD34 negative and PAS positive (CD34-/PAS+) staining (left panel). Representative image of VM negative tissue (right panel) (magnification, 400 ×); scale bars represent 25 μm. B. Representative images of IHC staining of p-ERK1/2 high (left panel) or low expression (right panel) in PDAC tissues (magnification, 400 ×); scale bars represent 25 μm. C. Kaplan-Meier survival curve demonstrated that VM-positive tissues was significantly related to poor prognosis (P=0.021). D. Matrigel tube formation assay was performed to evaluate the VM capacity in seven cell lines. Formation of tubular network structures on Matrigel by HUVECs compared with PDAC cells (magnification, 100 ×); scale bars represent 100 μm. E. Histogram showing the numbers of VM channels in the different cells.

pression" (≥6). The sections were viewed and subjected to careful identification by two trained pathologists.

Matrigel tube formation assay

The Matrigel tube formation assay is a classic technique applied to identify the VM capacity of cancer cells in vitro. Ninety-six-well culture plates were coated with pre-cooled Matrigel (80 μl/well) and then incubated at 37°C for 2 h. To investigate the effect of JQ1 and SCH772984 on VM, the cells were treated with JQ1 (1 μM, 2 μM or 5 μM) or SCH772984 (1 μM, 5 μM or 10 μM) for 24 h. Then, 100 μl of cell suspension without serum (2×10^4 cells) were seeded onto the surface of the Matrigel and incubated at 37°C for 6 h. The cultures were monitored and imaged under a microscope. VM formation was quantified as the number of

Table 1. Association of VM expression with clinicopathological characteristics in 76 PDAC patients

Characteristics	No. of patients		VM expression		*P*-value
	n	%	Negative	Positive	
Age (years)					0.362
≤ 60	23	30.3	7	16	
> 60	53	69.7	11	42	
Gender					0.733
Male	49	64.5	11	38	
Female	27	35.5	7	20	
Clinical stage					0.049*
Early stages (≤ Ia)	12	15.8	6	6	
Advanced stages (> Ia)	64	84.2	12	52	
Invasion depth					0.759
T1 + T2	17	22.4	5	12	
T3 + T4	59	77.6	13	46	
Lymph nodes metastasis					0.023*
N0 (negative)	33	43.4	12	21	
N1 (positive)	43	56.6	6	37	
Distant metastasis					0.567
M0 (Absent)	72	94..7	18	54	
M1 (Present)	4	5.3	0	4	
Tumor differentiation					0.233
Well, moderate	51	67.1	10	41	
Poor	25	32.9	8	17	
Tumor location					0.081
Head, neck	39	51.3	6	33	
Body, tail	37	48.7	12	25	
Nervous invasion					0.077
Negative	25	32.9	9	16	
Positive	51	67.1	9	42	
Vessal invasion					0.397
Negative	65	85.5	17	48	
Positive	11	14.5	1	10	

*P<0.05 indicates a significant association among the variables.

complete structures per field in five randomly selected fields.

Western blotting

The cells were collected after JQ1 or SCH-772984 treated for 48 h. Samples of 50 μg of protein were subsequently applied to 10% SDS-PAGE and transferred to nitrocellulose membranes. The membranes were blocked in 5% bovine serum albumin (BSA) for 1 h, incubated with the primary antibody overnight at 4°C, washed, and incubated with the secondary antibody (1:2000) for approximately 1 h at room temperature. The immunoblot images were quantitated using ImageJ.

Tumorigenicity assays in vivo

The animal experiments were conducted according to the guidelines for animal experimentation and were approved by the Experimental Animal Ethics Committee of Shanghai Jiao Tong University. PANC-1 (2×10^6 cells) was subcutaneously injected into 4-week-old male BALB/c nude mice. When the tumor volumes reached 200 mm^3, the mice were randomly divided into a control group, low-dose (50 mg/kg) and high-dose (80 mg/kg) (+)JQ1 groups. The experimental group of mice was orally administered JQ1 at these doses once a day, and the control group of mice was intraperitoneally administered an equal volume of (-)JQ1. The mice were sacrificed, and the tumors were excised, weighed, harvested and embedded in paraffin. The expressions of VM and p-ERK1/2 were detected by CD34/PAS and IHC staining respectively.

Statistical analyses

The results were repeated in at least three separate experiments. The data are expressed as the means ± SD. Statistical comparisons were carried out using one-way analysis of variance, which revealed significant differences between groups. The X^2 test and Fisher's exact test were used to analyze the correlation between the clinicopathologic characteristics and VM expression as appropriate. Overall survival (OS) was defined as the interval from date of diagnosis until death from any cause. Data were censored for living patients and patients lost between follow-ups. The OS was estimated using the Kaplan-Meier method and compared using the Log-rank test. Significant variables were further analyzed by multivariate analysis to test for independent prognosis. Bivariate correlations between variable factors were calculated by Spearman rank correlation coeffi-

Table 2. Summary of univariate and multivariate Cox regression analysis of overall survival duration in all PDACs

Variables	Univariate analysis			Multivariate analysis		
	HR	(95% CI)	P	HR	(95% CI)	P
VM in cancer tissues						
Negative	1			1		
Positive	2.502	1.114-5.623	0.026*	2.484	1.034-5.966	0.042*
Age (years)						
≤ 60	1					
> 60	0.765	0.415-1.409	0.39			
Gender						
Male	1					
Female	1.116	0.600-2.076	0.728			
Clinical stage						
Early stages (≤ Ia)	1			1		
Advanced stages (> Ia)	4.059	1.255-13.123	0.019*	3.155	0.899-11.078	0.073
Invasion depth						
T1 + T2	1					
T3 + T4	1.937	0.864-4.342	0.109			
Lymph nodes metastasis						
N0 (negative)	1					
N1 (positive)	1.264	0.699-2.284	0.439			
Distant metastasis						
M0 (Absent)	1					
M1 (Present)	0.597	0.144-2.468	0.476			
Tumor differentiation						
Well, moderate	1			1		
Poor	1.963	1.084-3.553	0.026*	2.858	1.445-5.653	0.003*
Tumor location						
Head, neck	1					
Body, tail	1.541	0.854-2.779	0.151			
Nervous invasion						
Negative	1			1		
Positive	2.018	1.020-3.993	0.044*	1.111	0.537-2.298	0.777
Vessal invasion						
Negative	1			1		
Positive	4.107	1.978-8.528	<0.001*	4.456	1.879-10.571	0.001*

HR hazard ratio, 95% CI 95% confidence interval. *P<0.05 indicates a significant association among the variables.

cients. *P*-values <0.05 were considered statistically significant.

Results

The relationship between VM expression and the clinical factors of PDAC patients

We first assessed the VM expression by CD-34/PAS double-staining in 76 PDAC tissue specimens. The VM characteristics were as defined as CD34-negative and PAS-positive (CD34-/PAS+) vascular-like patterns, which were composed of cancer cells instead of endothelial cells (**Figure 1A**). Next, we examined the relationship between VM expression and clinical factors in PDAC patients. The results demonstrated that VM-positive structures were correlated with clinical stage (P= 0.049) and lymph node metastasis (P=0.023) (**Table 1**). However, the VM expression was not correlated with age, gender, invasion depth, tumor differentiation or tumor location and so on.

Table 3. Association between VM and p-ERK1/2 expression in PDAC tissues

Tumor tissues sample	VM expression		Correlation coefficient	*P*-value
	Negative	Positive		
p-ERK1/2 Low	15	20	0.401	<0.001*
p-ERK1/2 High	3	38		

*P<0.05 indicates a significant association among the variables.

VM positive predicts poor patient outcomes

The prognostic implication of VM in PDAC was subsequently analyzed. Moreover, Kaplan-Meier survival curves showed that the OS was significantly worse in "VM positive" PDAC patients than in "VM negative" patients (P=0.021), which demonstrated that VM positivity was associated with a poor prognosis in PDAC patients (**Figure 1C**). In addition, univariate analysis indicated that VM expression, clinical stage, tumor differentiation, neural invasion and vessel invasion were correlated with patients' OS (all P<0.01; **Table 2**). Using multivariate Cox regression analysis (**Table 2**), VM was identified as a negative prognostic factor for PDAC patients in OS (hazard ratio [HR] 2.484; 95% confidence interval [CI] 1.034-5.966; P=0.042).

VM expression is positively correlated with p-ERK1/2 in PDAC

Increasing evidence shows that the ERK1/2 signaling pathways play critical roles in VM formation in various tumors [9-11]. Therefore, we first assessed the p-ERK1/2 expression level by IHC staining in 76 PDAC tissue specimens and further explored the relationship between VM and p-ERK1/2 expression levels. The result showed that tumor tissues of VM positive patients showed higher p-ERK1/2 expression compared to that patient of VM negative (**Figure 1A**, **1B**). This data suggested a positive correlation between VM expression and p-ERK1/2 levels in PDAC specimens (P<0.001) (**Table 3**).

The ERK1/2 inhibitor SCH772984 prevents the development of VM by inhibiting MMP-2/9 expression in vitro

We above data have found that the VM expression positively correlated with p-ERK levels, and then we further verified whether the p-EKR1/2 inhibitor could reduce VM formation in vitro. First, we detected the VM capacity in six cell lines of PDAC. HUVECs were used as positive control. AsPC-1 and PANC-1 cells readily formed VM channels, whereas the other PDAC cells failed to form any tubes or networks (**Figure 1D**). Next, VM expression was further quantified in the different cell lines (**Figure 1E**). Therefore, we chose AsPC-1 and PANC-1 cells for use in the following experiments.

Further, we found that ERK1/2 inhibitor SCH-772984 significantly disrupted the formation of capillary-like structures in a dose-dependent manner in comparison with control group. And 10 μM SCH772984 completely inhibited VM formation (**Figure 2A**, **2B**). Western blot result showed that expression of p-ERK1/2, MMP-2 and MMP-9 was decreased than control group (**Figures 2C-F**, S1, S2). The above data indicate that inhibiting *ERK1/2* phosphorylation has a strong potentially destructive effect on VM formation in PDAC cell lines.

JQ1 prevents the development of VM by inhibiting ERK1/2-MMP-2/9 signaling pathway

Recently, Ana S. Leal et al. [17] reported that JQ1, a BET inhibitor, could inhibit tumor growth by decreasing the expression of p-ERK1/2 in PDAC cells. Therefore, we explored whether JQ1 could affect VM formation by suppressing the activation of p-ERK1/2 in PDAC. As shown in **Figure 3A**, the AsPC-1 cells produced relatively well-formed tubular structures in the negative control, whereas the VM formation ability of these cells were prominently inhibited in JQ1 treatment groups by a dose-dependent manner. Similar results were also observed in PANC-1 cells that were pretreated with above concentrations of JQ1 (**Figure 3B**). Western blotting results showed that JQ1 inhibited the activation of pERK1/2, MMP2 and MMP9, but had no significant effect on the level of total ERK1/2 protein (**Figures 3C-F**, S3, S4). Taken together, these results demonstrated that JQ1 inhibits VM formation via ERK1/2-MMP-2/9 signaling in PDAC cells.

JQ1 inhibits VM formation in vivo

To further identify the JQ1 in destroying VM formation in vivo, we established BALB/c xenograft nude mouse model with PANC-1 cells. As shown in **Figure 4A-C**, the mice that were treated with JQ1 (50 mg/kg or 80 mg/kg) demonstrated a reduced tumor volume and size

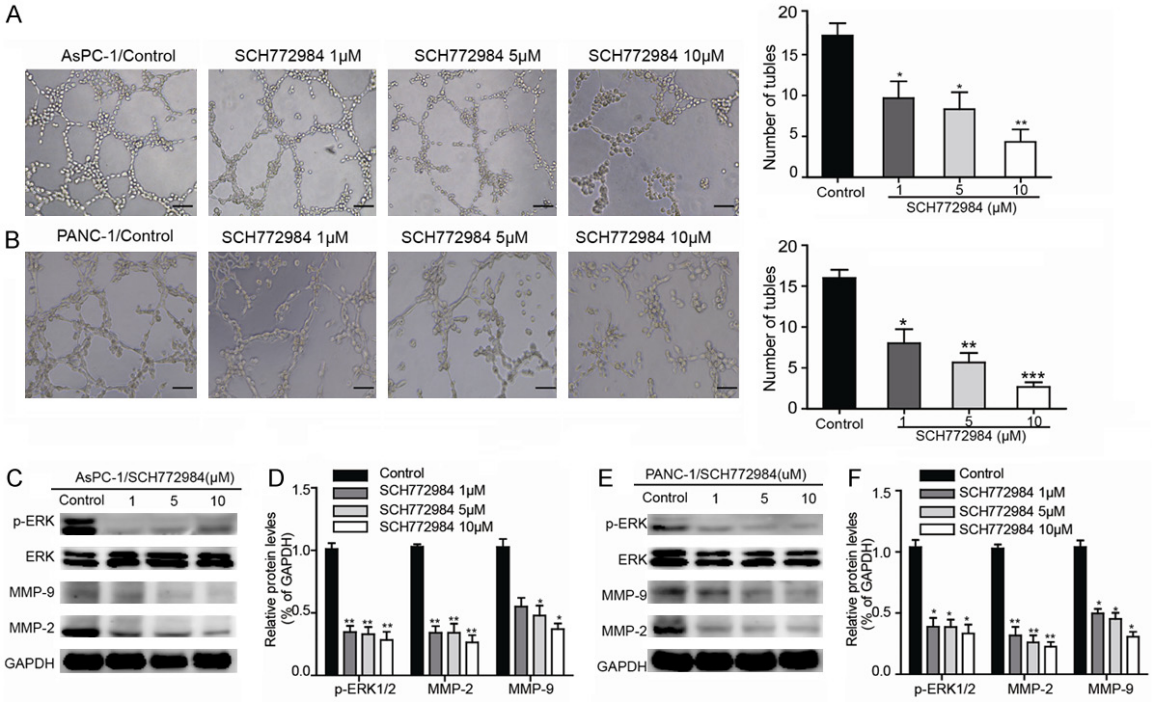

Figure 2. The ERK1/2 inhibitor SCH772984 suppresses VM formation and inhibits the expression of VM-associated key factors. A, B. Representative photographs showing the loop pattern on Matrigel culture (Ctrl) and the decreased number of tubules in the presence of 1, 5 or 10 μM SCH772984N in AsPC-1 and PANC-1 (magnification, 100 ×), scale bars represent 100 μm. The corresponding statistic results of the mean numbers of tube-like structures observed in five randomly chosen areas in each group. C, E. The p-ERK1/2, ERK1/2, MMP-2 and MMP-9 protein expression levels in each cell line were determined by western blot 48 h after SCH772984 treatment. D, F. Relative densities are presented as means ± SD of the fold change relative to the internal control. GAPDH was used as an internal control for protein loading. The data are shown as the means ± SD (triplicate assays); *P<0.05 vs Ctrl and **P<0.01 vs Ctrl.

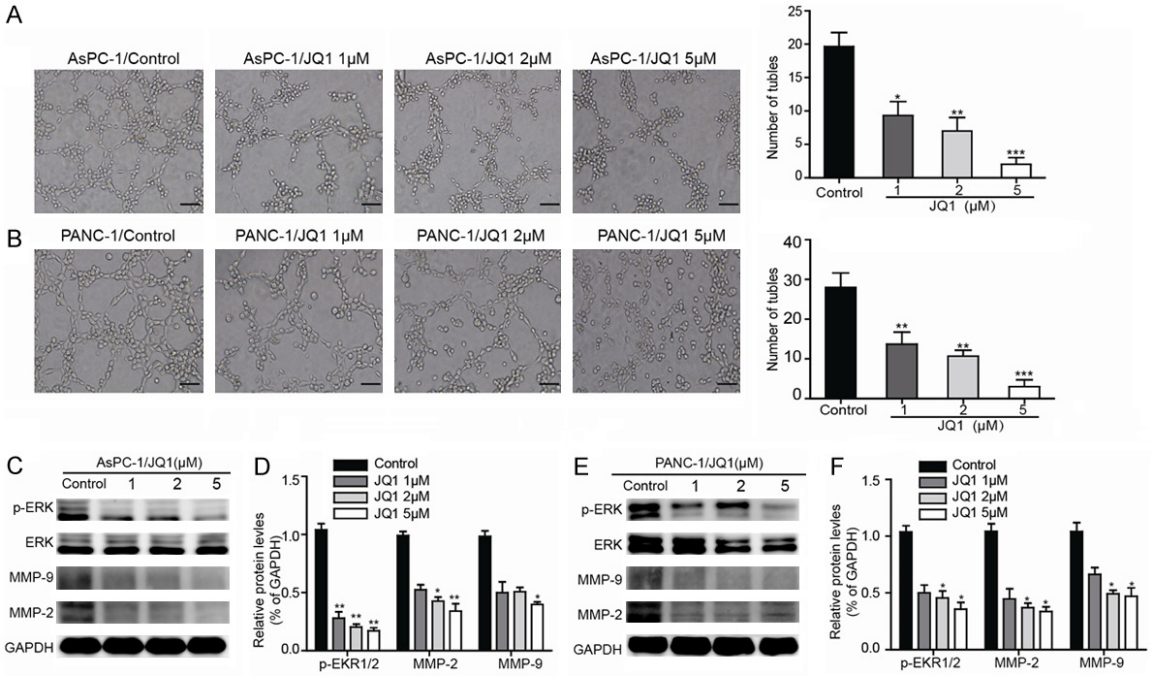

Figure 3. JQ1 destroys VM formation and decreases the expression of VM-associated key factors in vitro. A, B. AsPC-1 and PANC-1 cells were treated with the indicated concentration (1, 2, or 5 μM) of JQ1 for 24 h and then subjected

to a tube formation assay as described (magnification, 100 ×); scale bars represent 100 μm. Concentration-dependent effects of JQ1 on tube formation were determined by quantitative analysis of the mean number of tube-like structures formed in five randomly chosen areas in 3D cultures. C, E. After the cells were incubated with 0, 1, 2 or 5 μM JQ1 for 48 h, the protein expression levels of p-ERK1/2, ERK1/2, MMP-2, MMP-9 and GAPDH were determined by Western blot analysis. D, F. Relative densities are presented as the mean ± SD of the fold change relative to the internal control. GAPDH was used as an internal control for protein loading (triplicate assays). *P<0.05 vs Ctrl and **P<0.01 vs Ctrl.

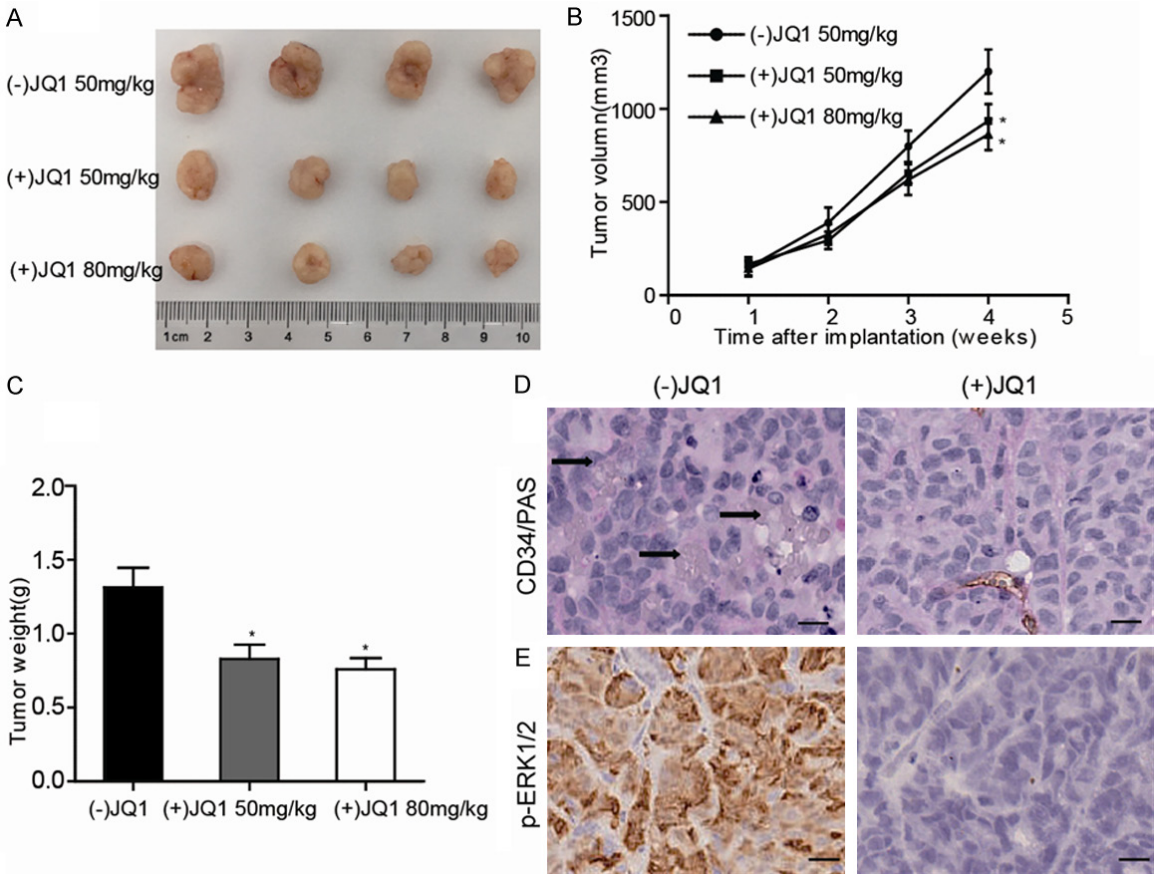

Figure 4. JQ1 inhibits VM expression in vivo. PANC-1 xenografts mice were treated with JQ1 (50 mg/kg daily) or JQ1 (80 mg/kg daily) for 30 days. A. The tumors were isolated and photographed. B. The tumor volumes in each group were monitored weekly and relative tumor volume curve showed that the growth of tumors in the JQ1 treatment groups were significantly slower than that of the tumors in the control group. C. The terminal weights were also determined. D, E. Immunohistochemical staining showed that the group with (+)JQ1 treatment groups exhibited a distinct decrease in VM formation (upper panel) and p-ERK1/2 expression (lower panel), black arrow indicates VM (CD34-/PAS+) in xenograft tumor (magnification, 400 ×); scale bars represent 25 μm; *P<0.05 vs Ctrl.

compared with the control mice. Meanwhile, we also detected the VM and p-ERK1/2 expressions in mice tumors. Interesting, the IHC analysis also revealed that VM and p-ERK1/2 expression levels were dramatically decreased in JQ1 treatment groups compared to that of control group (**Figure 4D**, **4E**). From the above, these results demonstrate that JQ1 had VM-destroying properties in PDAC via inhibiting ERK1/2-MMP2/9 signal pathway in vivo.

Discussion

VM is increasingly being accepted as an important promoter of cancer growth and metastasis in various aggressive tumors [16, 17], which suggests that VM may be a novel therapeutic target for cancer. Notably, VM expression has been demonstrated as an unfavorable survival factor and a marker of poor prognosis in many other cancers [18-20]. It is critical to seek a novel and more efficient agent to suppress the

formation of VM. However, the positive rate of VM expression and the clinical significance in patients with PDAC remain unclear. In this study, we have demonstrated that VM-positive is associated with an advanced stage and lymph node metastasis of PDAC and a shorter overall survival.

ERK1/2 has been recognized as a proto-oncogene and plays an important role in VM formation in various cancers. Li Y et al. [10] demonstrated that MALAT1 can promote tumorigenicity and metastasis by facilitating VM via the ERK/MMP signaling pathway in gastric cancer. Moreover, Zhang X et al. [21] found that netrin-1 can act as a pro-metastatic factor by enhancing VM, cell invasion and migration via ERK-mediated Epithelial-mesenchymal transition (EMT) process. Therefore, the ERK1/2-MMPs signal pathway was closely involved in the course of VM. Consequently, it's a practical way to inhibit VM formation by suppressing the activation of ERK1/2/MMPs signaling pathway. Therefore, we further detected the expression of p-ERK1/2 in PDAC tissues. Notably, our results revealed a positive correlation between VM and p-ERK1/2 expression in PDAC. Further, the ERK1/2 inhibitor SCH772984 demonstrated significantly destroyed VM structures, and inhibited MMP-2/9 protein levels, which were associated with VM formation in various cancers by regulating the stability [13]. The above data indicate that inhibiting ERK1/2 phosphorylation has a strong potentially destructive effect on VM formation in PDAC cell lines.

JQ1, a BET inhibitor, remains the most-studied drug in the class and is a promising epigenetic agent for the treatment of various tumors [22-24]. Furthermore, JQ1 has been well established in regulating cell cycle arrest, apoptosis, EMT and the stem cell nature of tumor cells, which were reported to be closely related to VM formation [25]. However, little is known about the roles of JQ1 as an anti-VM agent. Recently, JQ1 was also verified to inhibit tumor growth by decreasing the expression of p-ERK1/2 in PDAC cells [15]. Therefore, we further explored whether JQ1 could affect VM formation by suppressing the activation of p-ERK1/2 in PDAC both in vitro and in vivo. Here, we found that JQ1 significantly inhibited the key components of the ERK1/2 signaling pathway in vitro. Further analysis showed that the mice treated with JQ1 demonstrated slower tumor growth compared with the control mice by decreasing VM and p-ERK1/2 expression in vivo. Based on our results, JQ1 treatment was sufficient to abolish VM formation by blocking the phosphorylation of ERK1/2 and MMP-2/9 expressions, which indicated the potential role of JQ1 as a mediator of VM formation.

In summary, our findings revealed that VM-positive expression was not only identified as prognostic marker but also may serve as a therapeutic target in PDAC. Furthermore, our study provides a new perspective on the treatment of JQ1 could significantly disrupt the formation of VM via the ERK1/2-MMP-2/9 signal pathway both in vitro and in vivo. Thus, JQ1 could be further investigated as a promising anti-pancreatic cancer agent.

Acknowledgements

This study was supported in part by the National Natural Science Foundation of China (grant NO 81502017, 81502018, 81572315).

Disclosure of conflict of interest

None.

Address correspondence to: Liwei Wang and Feng Jiao, Department of Oncology, State Key Laboratory for Oncogenes and Related Genes, Renji Hospital, School of Medicine, Shanghai Jiaotong University, Shanghai Cancer Institute, Shanghai 200127, China. E-mail: liweiwang@shsmu.edu.cn (LWW); jiao_f@yeah.net (FJ)

References

[1] Binenbaum Y, Na'Ara S and Gil Z. Gemcitabine resistance in pancreatic ductal adenocarcinoma. Drug Resist Updat 2015; 23: 55-68.

[2] Hoem D, Straume O, Immervoll H, Akslen LA and Molven A. Vascular proliferation is associated with survival in pancreatic ductal adenocarcinoma. APMIS 2013; 121: 1037-1046.

[3] Rougier P, Riess H, Manges R, Karasek P, Humblet Y, Barone C, Santoro A, Assadourian S, Hatteville L and Philip PA. Randomised, placebo-controlled, double-blind, parallel-group phase III study evaluating aflibercept in patients receiving first-line treatment with gemcitabine for metastatic pancreatic cancer. Eur J Cancer 2013; 49: 2633-2642.

[4] Sun H, Zhang D, Yao Z, Lin X, Liu J, Gu Q, Dong X, Liu F, Wang Y, Yao N, Cheng S, Li L and Sun S. Anti-angiogenic treatment promotes triple-

negative breast cancer invasion via vasculogenic mimicry. Cancer Biol Ther 2017; 18: 205-213.
[5] Qiao L, Liang N, Zhang J, Xie J, Liu F, Xu D, Yu X and Tian Y. Advanced research on vasculogenic mimicry in cancer. J Cell Mol Med 2015; 19: 315-326.
[6] Williamson SC, Metcalf RL, Trapani F, Mohan S, Antonello J, Abbott B, Leong HS, Chester CP, Simms N, Polanski R, Nonaka D, Priest L, Fusi A, Carlsson F, Carlsson A, Hendrix MJ, Seftor RE, Seftor EA, Rothwell DG, Hughes A, Hicks J, Miller C, Kuhn P, Brady G, Simpson KL, Blackhall FH and Dive C. Vasculogenic mimicry in small cell lung cancer. Nat Commun 2016; 7: 13322.
[7] Shen Y, Quan J, Wang M, Li S, Yang J, Lv M, Chen Z, Zhang L, Zhao X and Yang J. Tumor vasculogenic mimicry formation as an unfavorable prognostic indicator in patients with breast cancer. Oncotarget 2017; 8: 56408-56416.
[8] Lv J, Sun B, Sun H, Zhang Y, Sun J, Zhao X, Gu Q, Dong X and Che N. Significance of vasculogenic mimicry formation in gastric carcinoma. Oncol Res Treat 2017; 40: 35-41.
[9] Huang B, Xiao E and Huang M. MEK/ERK pathway is positively involved in hypoxia-induced vasculogenic mimicry formation in hepatocellular carcinoma which is regulated negatively by protein kinase A. Med Oncol 2015; 32: 408.
[10] Li Y, Wu Z, Yuan J, Sun L, Lin L, Huang N, Bin J, Liao Y and Liao W. Long non-coding RNA MALAT1 promotes gastric cancer tumorigenicity and metastasis by regulating vasculogenic mimicry and angiogenesis. Cancer Lett 2017; 395: 31-44.
[11] Liu ZJ, Zhou YJ, Ding RL, Xie F, Fu SZ, Wu JB, Yang LL, Wen QL. In vitro and in vivo apatinib inhibits vasculogenic mimicry in melanoma MUM-2B cells. PLoS One 2018; 13: e0200845.
[12] Lin H, Pan JC, Zhang FM, Huang B, Chen X, Zhuang JT, Wang H, Mo CQ, Wang DH, Qiu SP. Matrix metalloproteinase-9 is required for vasculogenic mimicry by clear cell renal carcinoma cells. Urol Oncol 2015; 33: 168, e9-16.
[13] Li Y, Sun B, Zhao X, Wang X, Zhang D, Gu Q, Liu T. MMP-2 and MMP-13 affect vasculogenic mimicry formation in large cell lung cancer. J Cell Mol Med 2017; 21: 3741-3751.
[14] Ferri E, Petosa C, McKenna CE. Bromodomains: structure, function and pharmacology of inhibition. Biochem Pharmacol 2016; 106: 1-18.
[15] Leal AS, Williams CR, Royce DB, Pioli PA, Sporn MB and Liby KT. Bromodomain inhibitors, JQ1 and I-BET 762, as potential therapies for pancreatic cancer. Cancer Lett 2017; 394: 76-87.
[16] Zhang J, Qiao L, Liang N, Xie J, Luo H, Deng G and Zhang J. Vasculogenic mimicry and tumor metastasis. J BUON 2016; 21: 533-541.
[17] Wu ZZ, Chen LS, Zhou R, Bin JP, Liao YL and Liao WJ. Metastasis-associated in colon cancer-1 in gastric cancer: beyond metastasis. World J Gastroenterol 2016; 22: 6629-6637.
[18] Gong W, Sun B, Zhao X, Zhang D, Sun J, Liu T, Gu Q, Dong X, Liu F, Wang Y, Lin X and Li Y. Nodal signaling promotes vasculogenic mimicry formation in breast cancer via the Smad2/3 pathway. Oncotarget 2016; 7: 70152-70167.
[19] Cao Z, Bao M, Miele L, Sarkar FH, Wang Z, Zhou Q. Tumour vasculogenic mimicry is associated with poor prognosis of human cancer patients: a systemic review and meta-analysis. Eur J Cancer 2013; 49: 3914-3923.
[20] Liang J, Yang B, Cao Q, Wu X. Association of vasculogenic mimicry formation and CD133 expression with poor prognosis in ovarian cancer. Gynecol Obstet Invest 2016; 81: 529-536.
[21] Zhang X, Cui P, Ding B, Guo Y, Han K, Li J, Chen H, Zhang W. Netrin-1 elicits metastatic potential of non-small cell lung carcinoma cell by enhancing cell invasion, migration and vasculogenic mimicry via EMT induction. Cancer Gene Ther 2018; 25: 18-26.
[22] Zhu X, Enomoto K, Zhao L, Zhu YJ, Willingham MC, Meltzer P, Qi J and Cheng SY. Bromodomain and extraterminal protein inhibitor JQ1 suppresses thyroid tumor growth in a mouse model. Clin Cancer Res 2017; 23: 430-440.
[23] Shimamura T, Chen Z, Soucheray M, Carretero J, Kikuchi E, Tchaicha JH, Gao Y, Cheng KA, Cohoon TJ, Qi J, Akbay E, Kimmelman AC, Kung AL, Bradner JE and Wong KK. Efficacy of BET bromodomain inhibition in Kras-mutant non-small cell lung cancer. Clin Cancer Res 2013; 19: 6183-6192.
[24] Garcia PL, Miller AL, Kreitzburg KM, Council LN, Gamblin TL, Christein JD, Heslin MJ, Arnoletti JP, Richardson JH, Chen D, Hanna CA, Cramer SL, Yang ES, Qi J, Bradner JE and Yoon KJ. The BET bromodomain inhibitor JQ1 suppresses growth of pancreatic ductal adenocarcinoma in patient-derived xenograft models. Oncogene 2016; 35: 833-845.
[25] Sun B, Zhang D, Zhao N and Zhao X. Epithelial-to-endothelial transition and cancer stem cells: two cornerstones of vasculogenic mimicry in malignant tumors. Oncotarget 2017; 8: 30502-30510.

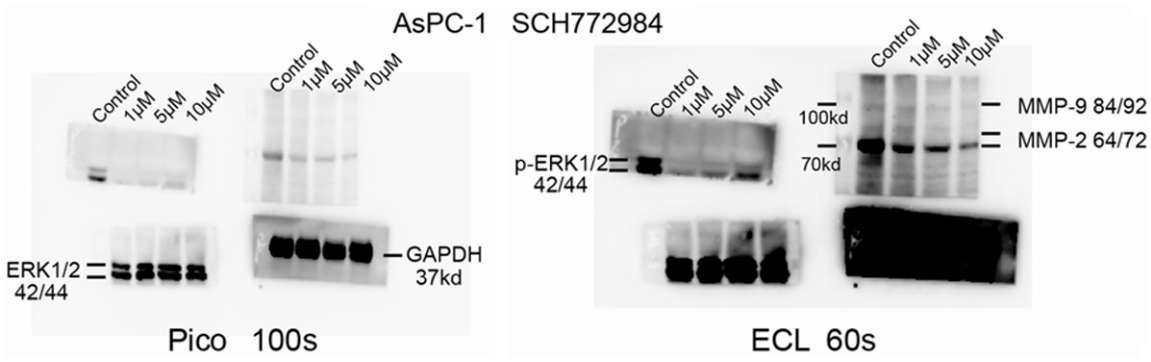

Figure S1. The ERK1/2 inhibitor SCH772984 suppresses VM formation and inhibits the expression of VM-associated key factors in AsPC-1. The western images were exposed in Pico substrate solution for 100 s (left panel) and ECL for 60 s (lower panel).

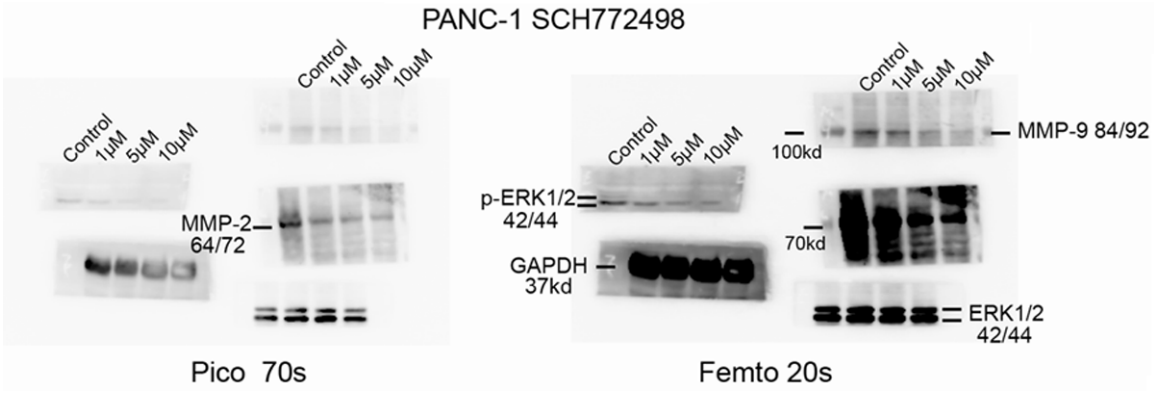

Figure S2. SCH772984 suppresses VM formation and inhibits the expression of VM-associated key factors in PANC-1. The western images were exposed in Pico substrate solution for 70 s (left panel) and Femto for 20 s (lower panel).

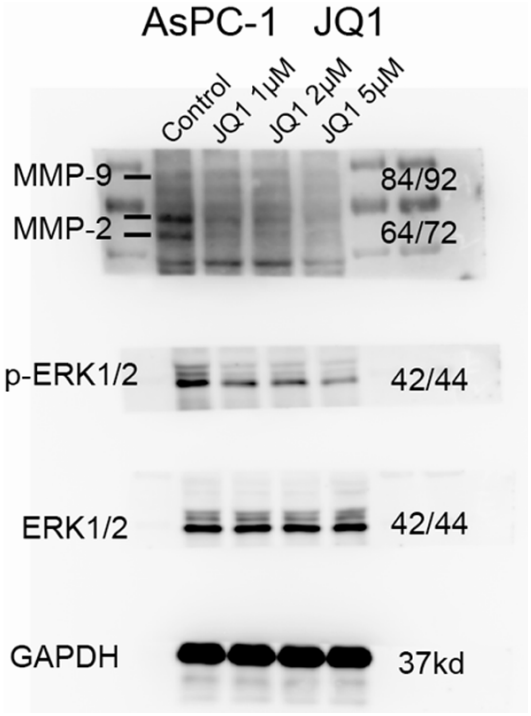

Figure S3. JQ1 suppresses VM-like network formation and inhibits the expression of VM-associated key factors in AsPC-1. The western images were exposed by chemical exposure.

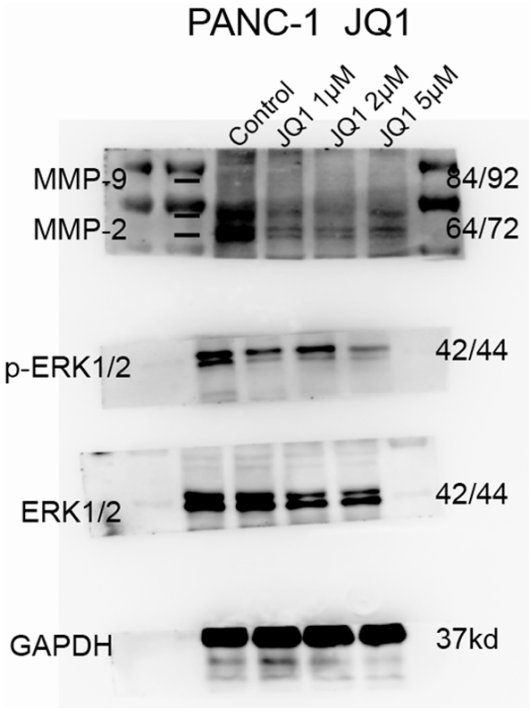

Figure S4. JQ1 suppresses VM-like network formation and inhibits the expression of VM-associated key factors in PANC-1. The western images were exposed by chemical exposure.